

## Electrical characteristics of rat skeletal muscle in immaturity, adulthood and after sciatic nerve injury, and their relation to muscle fiber size

This article has been downloaded from IOPscience. Please scroll down to see the full text article.

2009 Physiol. Meas. 30 1415

(<http://iopscience.iop.org/0967-3334/30/12/009>)

View [the table of contents for this issue](#), or go to the [journal homepage](#) for more

Download details:

IP Address: 128.103.149.52

The article was downloaded on 24/02/2011 at 15:01

Please note that [terms and conditions apply](#).

## Electrical characteristics of rat skeletal muscle in immaturity, adulthood and after sciatic nerve injury, and their relation to muscle fiber size

Mohammad A Ahad, P Michelle Fogerson, Glenn D Rosen,  
Pushpa Narayanaswami and Seward B Rutkove<sup>1</sup>

Division of Neuromuscular Diseases, Department of Neurology, Harvard Medical School,  
Beth Israel Deaconess Medical Center, 330 Brookline Avenue, Boston, MA 02215, USA

E-mail: [srutkove@bidmc.harvard.edu](mailto:srutkove@bidmc.harvard.edu)

Received 16 July 2009, accepted for publication 12 October 2009

Published 4 November 2009

Online at [stacks.iop.org/PM/30/1415](http://stacks.iop.org/PM/30/1415)

### Abstract

Localized impedance methods can provide useful approaches for assessing neuromuscular disease. The mechanism of these impedance changes remains, however, uncertain. In order to begin to understand the relation of muscle pathology to surface impedance values, 8 immature rats, 12 mature rats and 8 mature rats that had undergone sciatic crush were killed. Measurement was made on tissue from the gastrocnemius muscle from each animal in an impedance cell, and the conductivity and relative permittivity of the tissue were calculated in both the longitudinal and transverse directions for frequencies of 2 kHz to 1 MHz. In addition, quantitative histological analysis was performed on the tissue. Significant elevations in transverse conductivity and transverse relative permittivity were found with animal growth, but longitudinal values showed no difference. After sciatic crush, both transverse and longitudinal conductivity increased significantly, with no change in the relative permittivity in either direction. The frequency dependence of the values also changed after nerve injury. In the healthy animals, there was a strong linear relation between measured conductivity and relative permittivity with cell area, but not for the sciatic crush animals. These results provide a first step toward developing a comprehensive understanding of how the electrical properties of muscle alter in neuromuscular disease states.

Keywords: muscle, electrical impedance, conductivity, permittivity, dielectric

<sup>1</sup> Author to whom any correspondence should be addressed.

## 1. Introduction

Electrical impedance myography (EIM) is an electrophysiologic technique for the assessment of muscle that depends upon the surface application of high-frequency electrical current to muscles and the measurement of subsequent voltage patterns (Rutkove *et al* 2002, 2009). Although still under refinement, the technique offers the promise of a useful, non-invasive means for the evaluation of neuromuscular disease, and to date, we have identified changes in the major EIM parameters, the resistance, reactance and phase in a variety of disease states (Rutkove *et al* 2005, 2007, Tarulli *et al* 2005). In addition, we have also observed that certain impedance patterns are more predictive of neurogenic disease and others more predictive of myopathic disease (Garmirian *et al* 2009).

For the most part, our research has focused on performing measurements predominantly in patients, correlating EIM changes to clinical parameters (Tarulli *et al* 2005, Rutkove *et al* 2007). Recently, however, we have initiated a program of reverse translational research, applying EIM to rat models of neuromuscular disease in order to assist in better identifying the mechanistic underpinnings of the observed changes in humans (Nie *et al* 2006, Ahad and Rutkove 2009). We have been able to establish that highly stable EIM data can be acquired from rats by the time they reach about 14 weeks of age and that EIM is sensitive to changes produced by sciatic nerve crush (Ahad and Rutkove 2009).

One major advantage of performing animal studies is that we can kill the animals and evaluate the muscle histologically in order to determine how changes in muscle structure and composition after injury contributes to measured surface EIM data. Equally important, by obtaining actual muscle tissue, we are also able to assess the actual electrical properties—the muscle's inherent electrical conductivity and its permittivity (Epstein and Foster 1983). Ultimately, by connecting these values to the surface measurements via the use of finite element analysis, it will be possible to model the changes observed in the rats. In this study, we report our initial efforts in that direction as we measure the electrical properties of the rat gastrocnemius muscle in healthy immature and mature animals and in adult animals after sciatic crush and then relate these findings to quantified histological measures.

## 2. Methods

### 2.1. Rats

Given the potential value of this research in the diagnosis and treatment of a variety of human neuromuscular conditions, this animal work was approved by the Institutional Animal Care and Use Committee of the Beth Israel Deaconess Medical Center, Boston, MA. A total of 28 rats were studied: 8 immature rats (weighing 140–160 g) and 20 mature rats (weighing 420–480 g), of which 8 underwent sciatic nerve crush. All were male Wistar rats obtained from Charles River Laboratories, Wilmington, MA, and were acclimated for 48 h after arrival at our animal facility before any measurements were obtained. Animals were fed Harlan Teklad Rodent Diet #7964. In the eight sciatic crush animals, an incision was made proximally in the thigh and the sciatic nerve exposed, being careful not to disturb surrounding tissues, with the animal anesthetized under isoflurane. A 1 mm length segment of nerve was then crushed using a jeweler's forceps by applying 3–4 MPa pressure for approximately 30 s. The incisions were then sutured closed and the animals were allowed to recover until they were killed 1–2 weeks later. Buprenorphine was administered at a dose of 0.5 mg kg<sup>-1</sup> every 24 h for 2 days after surgery via intraperitoneal injection to control pain.

## 2.2. Needle electromyography

Limited needle electromyography (EMG) of the lateral gastrocnemius to assess for the presence of fibrillation potentials was performed afterward to confirm that sufficient nerve injury had been achieved. A TECA Synergy T2 EMG Monitoring System (Viasys, Madison, WI) was used for recording via a standard concentric EMG needle.

## 2.3. Impedance measurement system

A lock in amplifier, Signal Recovery Model 7280, Advanced Measurement Technology Inc., Oak Ridge, TN, was used to supply ac currents from its 1 V reference output oscillator, and the selected voltage was fed to its input terminal through a high impedance and very low capacitance active probe (Model 1103 of Tektronix, Beaverton, OR) as previously described (Esper *et al* 2006). Instrument-interfacing software was written in Visual Basic to calculate resistance and reactance and also display and store recorded impedance data. The system was calibrated with resistor-capacitor circuits of known character, designed to mimic to the electrical properties of muscle; in addition, the system was also tested using 0.9%, 0.45%, 0.225% and 0.1125% saline solutions to confirm data consistency.

## 2.4. Measurements of the electrical constants

After obtaining surface impedance measurements over the gastrocnemius muscle (a foot flexor), as reported in Ahad and Rutkove 2009, and with the animals still under anesthesia, the skin overlying the leg was cut with scissors and the tissue dissected down to expose the entire gastrocnemius muscle. The animal was then killed via an overdose of intraperitoneal Nembutal<sup>®</sup> or FatalPlus<sup>®</sup>, and the entire gastrocnemius muscle was immediately excised at its proximal extent just below the knee and distally by cutting the gastrocnemius tendon at its insertion into the calcaneus. A superficial portion of this muscle, approximately 1 cm × 1 cm square of about 0.4 cm height was excised with a scalpel. The tissue was kept moist and warm by its being covered with 0.9% saline-saturated gauze under a heating lamp, maintaining the tissue at 36–37 °C. All animals were killed between 7 and 14 days after crush, with one to two being studied per day.

This tissue was then placed into a 1 cm × 1 cm × 2 cm plastic measuring cell between two stainless steel current electrodes with the fiber orientation perpendicular to the metal electrodes (providing longitudinal measurements), similar to the approach of Baumann *et al* (1997). The top of the cell was fitted with a removable plastic lid with four holes, each 2 mm apart from each other and with the outermost holes also 2 mm away from the edge of the cell. The current electrodes were 1 cm in width and 5 cm in length, and thus contacted entirely the two sides of the rectangular slab of muscle. Two disposable monopolar EMG needle electrodes of Viasys Healthcare (Ref# 902-DMG50) were used as two voltage-measuring electrodes. These two voltage electrodes were inserted through the holes of the plastic cover such that they just contacted the surface of the muscle, and measurements were made using the above system in the 2 kHz to 1 MHz range. The muscle was then rotated by 90° such that the muscle fibers were parallel to the stainless steel plates and measurements repeated (transverse measurements). To ensure consistent temperature, the entire cell was maintained at 37 °C through the use of a heating pad surrounding the cell. After measurements were completed, the muscle tissue was immediately frozen in isopentane cooled in liquid nitrogen for histological analysis (see below) and stored at –80 °C until ready for use.

## 2.5. Quantitative histology

The frozen tissue was cut in a Tissue Tek II cryostat (Miles Laboratories, Inc., Elkhart, IN) into 10  $\mu\text{m}$  thick sections and stained with hematoxylin and eosin (Dubowitz 1985). The same superficial section of gastrocnemius used for the impedance measurements was used for the histological analysis. The slides were chosen blind to the group, but based on their high-quality staining and good cross-sectional muscle fiber orientation. Given the time-consuming nature of the histological analysis, tissues from only the last eight consecutive healthy mature animals were used (in other words, four healthy mature animals' histology was not assessed, leaving all eight animals in each of the three groups).

Standard stereological measurements (Mayhew *et al* 1997) were made using a Zeiss Axiophot microscope with a LUDL motorized stage interfaced with a Dell Optiflex 380 computer running Stereo Investigator (MBF Biosciences, Inc., Williston, VT) software. This software allows a non-biased quantification of fiber sizes. After the investigator sets a series of initial parameters, including the section of tissue from which to choose cells, the system automatically and randomly selects groups of cells to count. A total of approximately 300 cells were evaluated from each animal. In order to further reduce the potential for any bias, the evaluator (PMF) was blinded as to the type of section (immature animal, adult healthy animal, sciatic crush animal). For each slide, a histogram of cell size (in cross-sectional area and diameter) is obtained.

## 2.6. Data analysis

**2.6.1. Calculation of electrical constants.** Resistance and reactance were measured from the muscle piece in a plexiglass cell. The measured complex impedance of the muscle can be written as

$$Z = R + jX. \quad (1)$$

Alternatively, the complex admittance is written as

$$Y = \frac{1}{Z} = G + j\omega C \quad (2)$$

where conductance  $G$  and capacitance  $C$  can be given as

$$G = \frac{R}{R^2 + X^2} \quad (3)$$

$$C = \frac{X}{(R^2 + X^2)\omega} \quad (4)$$

and  $\omega = 2\pi f$ . The muscle's inherent electrical properties, including its conductivity and permittivity, are related to conductance and capacitance, respectively, by a geometry factor,  $K$ , of the measuring system. In this case, the measuring system is the parallel plate current electrodes with two voltage-measuring needle electrodes. The conductivity,  $\sigma$ , is related to this geometry factor,  $K$ , as

$$\sigma = K \cdot G. \quad (5)$$

And relative permittivity,  $\epsilon_r$  is related as

$$\epsilon_r = \frac{K \cdot C}{\epsilon_o}. \quad (6)$$

The geometry factor is given as

$$K = \frac{d}{A} \quad (7)$$

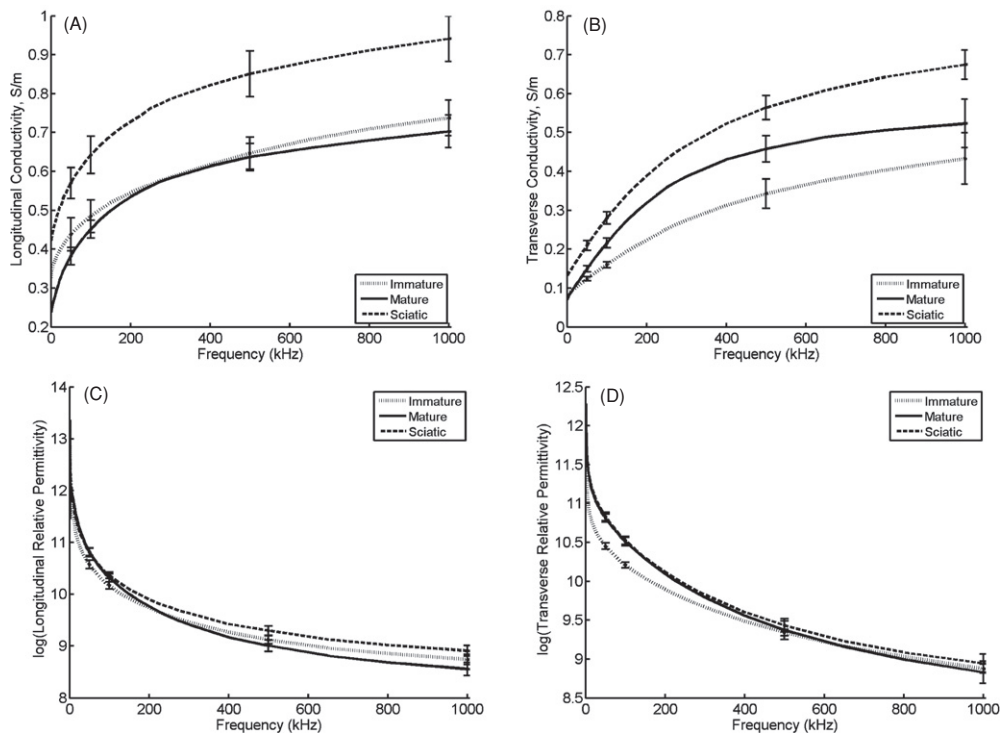


**Figure 1.** Conductivity and permittivity values ( $\pm$  standard error) at selected frequencies for the three groups of animals (immature, mature, and sciatic crush). (A) Longitudinal conductivity from 2 kHz to 1 MHz. (B) Transverse conductivity from 2 kHz to 1 MHz (note the different scales between (A) and (B)). (C) Log (longitudinal permittivity) from 2 kHz to 1 MHz. (D) Log (transverse permittivity) from 2 kHz to 1 MHz.

where  $A$  is the contact area of the muscle and the current electrode and  $d$  is the distance between the two needle electrodes.  $\epsilon_o$  is the permittivity of free space, which is given by  $8.85 \times 10^{-12} \text{ F m}^{-1}$ .

Using these equations, the conductivity and permittivity values for the section of each muscle in both the longitudinal and transverse directions were calculated. Data were plotted across the entire frequency spectrum of measurement from 2 kHz to 1 MHz and also reported at specific frequencies of 50 kHz, 100 kHz, 500 kHz and 1 MHz.

**2.6.2. Correlation of impedance data to muscle histology.** For each animal, the median, rather than mean muscle fiber size was measured since the distribution of fibers was sometimes skewed. Rank correlation (Spearman) was used to relate the measured dielectric constants for the muscle from each individual animal to the measured muscle fiber area. Comparisons of the two groups were made via standard  $t$ -tests as the group data were normally distributed with equal variances. Significance was kept at 0.05, two-tailed for all measurements. Statistical analyses were completed using SPSS (SPSS, Inc., Chicago, IL).

### 3. Results

#### 3.1. Changes in electrical constants in longitudinal and transverse directions

Figure 1 provides the average conductivity and relative permittivity data across the frequency spectrum in both the longitudinal and transverse directions for all three categories of animals:

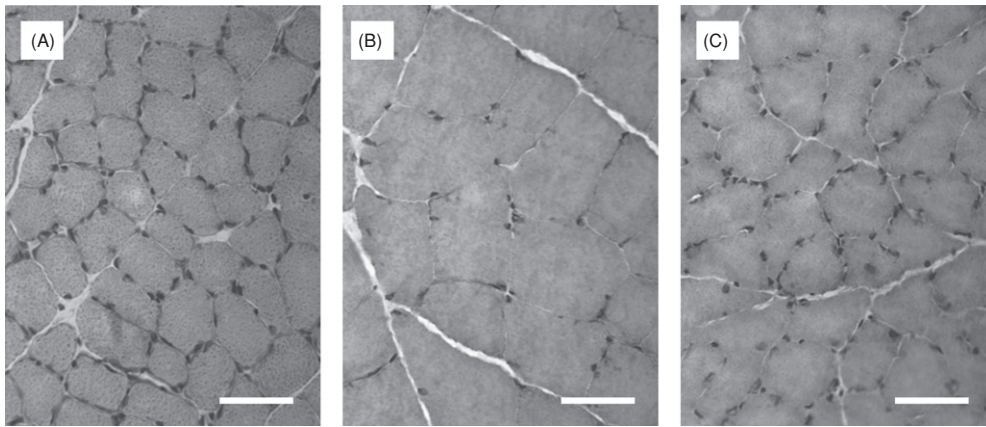


**Figure 2.** (A) Gastrocnemius muscle from an immature rat (40 $\times$ ), hematoxylin and eosin. (B) Gastrocnemius muscle from a mature rat (40 $\times$ ), hematoxylin and eosin. (C) Gastrocnemius muscle from a mature rat 2 weeks after sciatic crush (40 $\times$ ), hematoxylin and eosin. Bar = 50  $\mu\text{m}$ .

immature, mature and sciatic crush. Tables 1 and 2 provide statistical analyses at selected frequencies of 50 kHz, 100 kHz, 500 kHz and 1 MHz for these data. Conductivity in the longitudinal direction is similar between immature and mature animals. Likewise, permittivity in the longitudinal direction is not significantly different, although it is somewhat higher in the mature rats at low frequencies and lower in the mature rats at high frequencies. However, there are significant differences at most frequencies for both the transverse conductivity and relative permittivity, both being higher in the mature rats as compared to the immature.

When comparing the sciatic crush and the healthy mature animals, conductivity at all frequencies is higher in both transverse and longitudinal directions in the sciatic crush animals. Relative permittivity, although slightly higher in the crush animals at all but the lowest frequencies, is not significantly different.

With regard to our non-significant results for the comparisons between immature animals, we would expect to have a greater than 90% power to detect a  $0.16 \text{ S m}^{-1}$  difference in longitudinal conductivity and greater than 90% power to detect a difference of 1600 in longitudinal relative permittivity at 50 kHz. With regard to the non-significant comparisons between mature and crush animals, we would still have about the same power for the longitudinal conductivity measurements, but only about an 80% power to detect a difference of 12 000 in the longitudinal relative permittivity at 50 kHz.

### 3.2. Histological differences and relation to quantified measures

Immature rats had, on average ( $\pm$  standard error of the mean), a median muscle fiber area of  $1590 \pm 155 \mu\text{m}^2$  (range 902–2372  $\mu\text{m}^2$ ), whereas mature rats had, on average, a median muscle fiber area of  $3220 \pm 148 \mu\text{m}^2$  (range 2453–3756  $\mu\text{m}^2$ ); the crush animals had a median area of  $2082 \pm 60 \mu\text{m}^2$  (range 1967–2457  $\mu\text{m}^2$ ). The differences between mature and immature, and between mature and crush, were significant ( $p < 0.001$  for both comparisons). Examples of pathology are presented in figure 2 which shows prototypical data from an immature animal, a mature animal and a mature animal within 2 weeks of crush injury. Figure 3 shows scatter plots relating the different groups of animals to their muscle fiber areas.

**Table 1.** Longitudinal and transverse conductivities ( $\text{S m}^{-1}$ ) and permittivities ( $\pm$  standard error of the mean) of gastrocnemius muscle from immature and mature rats.

Frequency	50 kHz		100 kHz		500 kHz		1 MHz	
	$\sigma_L$	$\sigma_T$	$\sigma_L$	$\sigma_T$	$\sigma_L$	$\sigma_T$	$\sigma_L$	$\sigma_T$
Conductivity ( $\text{S m}^{-1}$ )								
Immature ( $N = 8$ )	$0.44 \pm 0.04$	$0.12 \pm 0.01$	$0.49 \pm 0.03$	$0.16 \pm 0.01$	$0.65 \pm 0.04$	$0.34 \pm 0.04$	$0.74 \pm 0.05$	$0.43 \pm 0.07$
Mature ( $N = 12$ )	$0.38 \pm 0.02$	$0.15 \pm 0.01$	$0.45 \pm 0.02$	$0.22 \pm 0.01$	$0.64 \pm 0.04$	$0.46 \pm 0.03$	$0.70 \pm 0.04$	$0.52 \pm 0.06$
Significance	ns	0.03	ns	0.002	ns	0.05	ns	ns
Permittivity	$\varepsilon_L$	$\varepsilon_T$	$\varepsilon_L$	$\varepsilon_T$	$\varepsilon_L$	$\varepsilon_T$	$\varepsilon_L$	$\varepsilon_T$
Immature ( $N = 8$ )	$39\,100 \pm 3200$	$34\,600 \pm 1400$	$26\,100 \pm 1900$	$27\,200 \pm 1000$	$9100 \pm 760$	$11\,400 \pm 460$	$6300 \pm 650$	$7200 \pm 400$
Mature ( $N = 12$ )	$47\,400 \pm 3100$	$47\,600 \pm 1900$	$29\,200 \pm 2200$	$35\,100 \pm 1400$	$8400 \pm 900$	$11\,400 \pm 1000$	$5300 \pm 600$	$7000 \pm 1100$
Significance	ns	0.001	ns	0.002	ns	ns	ns	0.04

$\sigma_L$ , longitudinal conductivity;  $\sigma_T$ , transverse conductivity;  $\varepsilon_L$ , longitudinal permittivity;  $\varepsilon_T$ , transverse permittivity.

**Table 2.** Longitudinal and transverse conductivities ( $\text{S m}^{-1}$ ) and permittivities ( $\pm$  standard error of the mean) of gastrocnemius muscle of healthy mature rats and rats within 2 weeks of sciatic nerve crush.

Frequency	50 kHz		100 kHz		500 kHz		1 MHz	
	$\sigma_L$	$\sigma_T$	$\sigma_L$	$\sigma_T$	$\sigma_L$	$\sigma_T$	$\sigma_L$	$\sigma_T$
Conductivity ( $\text{S m}^{-1}$ )								
Mature ( $N = 12$ )	$0.38 \pm 0.02$	$0.15 \pm 0.01$	$0.45 \pm 0.02$	$0.22 \pm 0.01$	$0.64 \pm 0.04$	$0.46 \pm 0.03$	$0.70 \pm 0.04$	$0.52 \pm 0.06$
Sciatic crush ( $N = 8$ )	$0.55 \pm 0.03$	$0.21 \pm 0.01$	$0.62 \pm 0.04$	$0.28 \pm 0.02$	$0.82 \pm 0.04$	$0.56 \pm 0.03$	$0.91 \pm 0.04$	$0.67 \pm 0.04$
Significance	0.004	0.002	0.009	0.006	0.004	0.02	0.007	0.04
Permittivity	$\epsilon_L$	$\epsilon_T$	$\epsilon_L$	$\epsilon_T$	$\epsilon_L$	$\epsilon_T$	$\epsilon_L$	$\epsilon_T$
Mature ( $N = 12$ )	$47\,400 \pm 3100$	$47\,600 \pm 1900$	$29\,200 \pm 2200$	$35\,100 \pm 1400$	$8400 \pm 900$	$11\,400 \pm 1000$	$5300 \pm 600$	$7000 \pm 1100$
Sciatic crush ( $N = 8$ )	$45\,800 \pm 2700$	$48\,500 \pm 2000$	$29\,900 \pm 1100$	$35\,800 \pm 1500$	$10\,500 \pm 1000$	$12\,200 \pm 1200$	$7100 \pm 800$	$7600 \pm 1000$
Significance	ns	ns	ns	ns	ns	ns	ns	ns

$\sigma_L$ , longitudinal conductivity;  $\sigma_T$ , transverse conductivity;  $\epsilon_L$ , longitudinal permittivity;  $\epsilon_T$ , transverse permittivity.

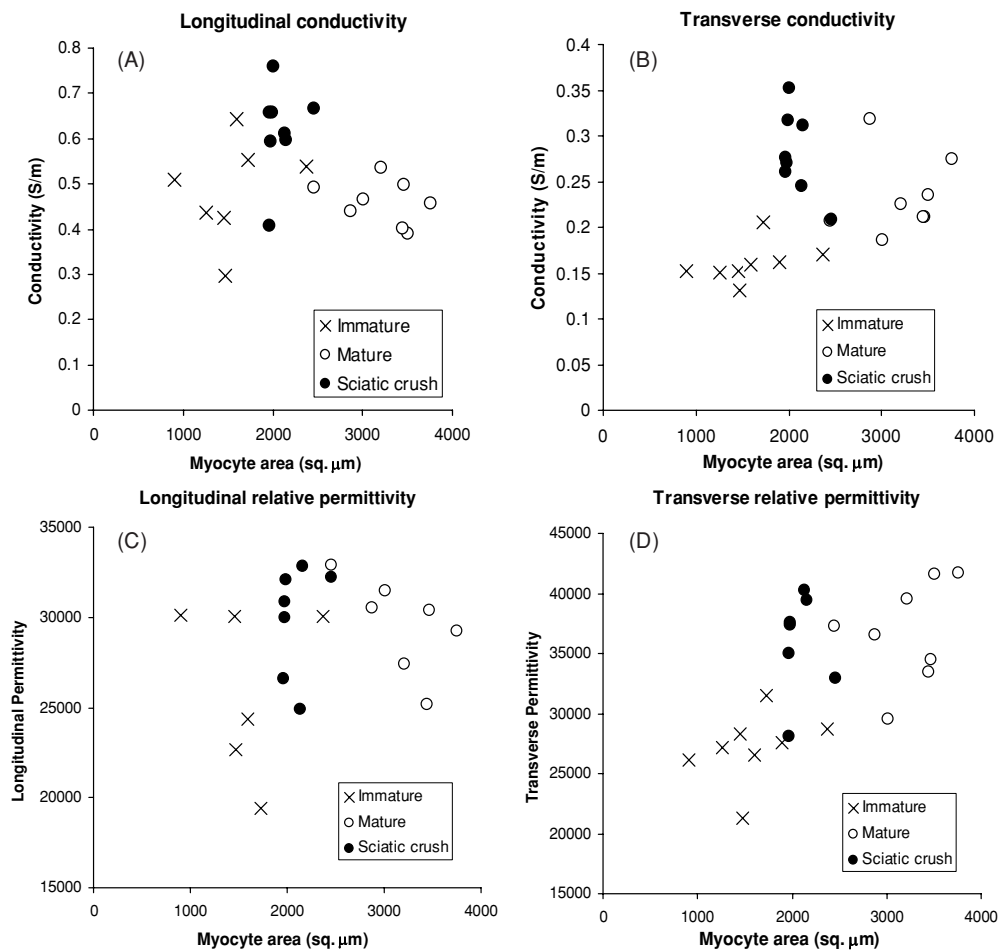


**Figure 3.** Scatterplots comparing the four electrical parameters to myocyte size. Each point represents the value from an individual animal. Note the prominent near-linear relation between transverse measurements and myocyte size in the immature and mature healthy animals and the lack of a relation in the longitudinal direction. In addition, crush animals show an elevation in conductivity in both longitudinal and transverse directions.

With growth from immaturity to maturity, the major changes observed are in the transverse measurements; both relative permittivity and conductivity increase linearly with muscle fiber area. Indeed, linear regression of all the non-crush animals (mature and immature) shows a strong relation (Spearman's  $\rho = 0.879$  ( $p < 0.001$ ) for transverse conductivity and muscle fiber area and Spearman's  $\rho = 0.865$  ( $p < 0.001$ ) for transverse permittivity). In comparison neither longitudinal parameter shows a significant correlation with muscle fiber size (Spearman's  $\rho = -0.129$ , NS for conductivity and  $0.198$ , NS for permittivity).

With crush, the major change is an increase in longitudinal conductivity as noted above and less so in transverse conductivity with no substantial change in the relative permittivity in either direction. It is worthwhile to highlight that although the muscle cells after crush are

more comparable in size to those of the immature animals, they have a higher rather than a lower transverse conductivity and relative permittivity (see figures 3(b) and (d)).

#### 4. Discussion

The data presented here confirm that significant changes in the electrical properties of skeletal muscle occur with rat growth and within 1–2 weeks after sciatic nerve injury. Indeed, our data for mature rat muscle corresponds well for values in rats and in other species as reported in a comprehensive review of the literature (Gabriel *et al* 1996). However, data on immature rats and on rat muscle after nerve injury have not been previously reported.

The changes in the electrical constants with animal growth likely reflect changes in the size of the myocytes, which is confirmed on our quantitative histological analysis and the remarkably strong linear relation between muscle fiber size and measured transverse conductivity and relative permittivity. Increasing the membrane area likely makes the muscle more easily polarized, thus leading to an increase in its relative permittivity. However, these changes may reflect more than just enlargement in the myocytes themselves, as the interstitium of the muscle also undoubtedly undergoes modification with growth. Other non-muscular factors could also play a role, including, for example, a maturing muscle vascular supply.

After sciatic nerve crush, there are very clear changes in the conductivity of the tissue, more so in the longitudinal than in the transverse direction, and non-significant changes in the relative permittivity. These changes may parallel those changes in the T2 signal observed on magnetic resonance imaging (MRI) of the muscle after nerve injury (Polak *et al* 1988, Wessig *et al* 2004). There are two causes offered for these T2 changes: (1) an increase in the extracellular space (Polak *et al* 1988) or (2) an increase in the size of the capillary bed (Wessig *et al* 2004). However, in the case of electrical impedance measurements, in addition to these two possibilities, changes in the membrane polarity or channel function could also play important roles.

Given that much of our clinical work is focused on measuring the surface impedance properties of the muscle in diseased states, we are also quite interested in understanding how the changes observed here relate to surface values. With surface measurements, we have generally observed reductions in the phase angle due to a simultaneous elevation in the resistance and a reduction in reactance of the tissue in diseased states (Rutkove *et al* 2002, Tarulli *et al* 2005, Rutkove *et al* 2007). However, the increasing conductivity of muscle we observed here would be expected to produce a reduction in the measured surface resistance. Thus, the observed elevation in surface resistance, at least in the case of recent nerve injury, is most likely a volumetric effect: a reduced area through which current can travel will increase the measured resistance. Although, presumably, the increased conductivity will offset this to some extent, it is insufficient. Similarly, the lack of any substantial change in the relative permittivity at 50 kHz in this study points to the likelihood that the observed effects are also mostly volumetric in nature, as clear reductions in the reactance are also generally observed in disease states.

A similar volumetric argument can be made for our surface data on immature animals in which we have also observed resistance being slightly higher in the younger animals and gradually decreasing and stabilizing as the animal reaches maturity (at about 350 g) (Ahad and Rutkove 2009). However, the same volumetric explanation cannot explain the elevated reactance of immature animals. Indeed, elevation in the measured surface reactance is consistent with the reduced relative permittivity of the tissue in the immature animals measured here.

Although these data suggest that single-frequency surface impedance measurements, for the most part, mainly provide a means for assessing muscle volume in nerve injury and with animal growth, the same may not be true for the behavior of the overall frequency spectrum. Indeed, the marked elevations in reactance values at high frequencies in patients with chronic neuromuscular disease (Esper *et al* 2006) suggest that the complexities of the frequency spectrum will reveal additional insights into tissue characteristics beyond a simple volumetric change. The complexity of these frequency-dependent changes is hinted at in figure 1 as the curves for the different groups of animals do not simply parallel each other. However, a full analysis of these frequency dependencies is beyond the scope of this study.

There are several limitations to this work worth highlighting. First, variability in the severity of the experimental crush lesion undoubtedly contributed to some of the variability in the observed measurements of the electrical constants. Second, although we attempted to perform these measurements as expeditiously as possible after each animal was killed, it is essentially impossible to know what these measurements would have shown if the muscle fibers were actually alive at the time of measurement. Accordingly, some caution must be exercised when comparing these values to those obtained with surface measurements on a living animal. Third, we are dealing with relatively small sizes of tissue in the normal rat and these tissue sizes become even smaller when the rats are immature or there is crush injury. Since the calculation of these constants requires a careful size measurement of the muscle, this undoubtedly also contributes to some of the observed variation. Fourth, even modest variations in the moistness of the tissue may contribute noise. We attempted to assure that all samples were treated identically, but this too is clearly subject to some variation. Finally, some variation in the size of the muscle fibers due to the shrinkage artifact may also have occurred due to our inability to pin or otherwise secure the tissue immediately after its removal from the animal; however, no obvious shrinkage was observed on histological analysis.

The main focus of this work was the correlation of muscle fiber electrical properties to muscle fiber size. We specifically did not attempt to evaluate fiber-type distributions or attempt to correlate these distributions to the changes in conductivity or relative permittivity. Although a potentially important question, as it is unknown whether fiber type actually impacts the electrical conductivity and permittivity of individual muscle fibers, pursuing that question as part of this study would have not been ideal. In order to answer this question most effectively, a study correlating the electrical properties of multiple muscles with different fiber type proportions in a group of adult healthy rats would be far more informative since muscle fiber size could be kept constant. Second, we were interested in evaluating acute changes in the muscle after nerve injury, and over the short time period evaluated here, limited reinnervation of the gastrocnemius muscle would have occurred and thus limited or inconsistent changes in fiber type would be expected, making the results of such an analysis even more uncertain. Nonetheless, this remains a very important question and will be pursued separately as part of our future planned work.

In addition to these limitations, the relevance of these initial rat-based studies to our human data needs to be considered. While the changes do mimic human nerve injury, much of our human studies, by necessity, have been in individuals with chronic not acute or subacute injuries. For example, we have reported findings in patients with chronic radiculopathy, amyotrophic lateral sclerosis and polio (Rutkove *et al* 2002, 2005, 2007). Thus, in order to specifically address this question, it will be necessary to study the time course of changes over a several month period. It is very possible that the early elevations in conductivity seen here might reverse as the muscle develops increased interstitial fat and connective tissue with loss of free water.

In summary, we have shown that muscle inherent conductivity and relative permittivity changes with growth and after sciatic nerve crush. In order to more fully apply impedance methods to neuromuscular disease states, it will be necessary to build upon the basic foundation laid out here by studying additional disease models, including models of disuse atrophy, muscular dystrophy, toxic myopathy and neurodegenerative diseases, including ALS. We also plan to incorporate the data obtained here into finite element models to better understand how the muscle's electrical properties relate to the observed surface measurements. For example, using the results of this work, it may be possible to more effectively interpret surface impedance data for diagnostic purposes. Alternatively, it may provide a new approach for muscle tissue evaluation by assessing its electrical properties in addition to its pathology.

## 5. Conclusion

We have studied the electrical properties of skeletal muscle in immature rats, mature rats, and mature rats after sciatic nerve injury and have correlated these values with muscle fiber diameter. Both transverse conductivity and relative permittivity increase with increasing muscle fiber diameter in healthy rats. Sciatic crush has a minimal effect on the relative permittivity of the tissue, but increases its conductivity in both orientations significantly. The frequency dependence of these values also changes with growth and after nerve injury.

## Acknowledgments

The authors thank Professors Carl Shiffman and Ronald Aaron of Northeastern University for their support and for the development of the system used to make these measurements. This study was funded by the National Institutes of Health Grant RO1-NS055099.

## References

- Ahad M and Rutkove S B 2009 Electrical impedance myography at 50 kHz in the rat: technique, reproducibility, and the effects of sciatic injury and recovery *Clin. Neurophys* **120** 1534–8
- Baumann S B, Wozny D R, Kelly S K and Meno F M 1997 The electrical conductivity of human cerebrospinal fluid at body temperature *IEEE Trans. Biomed. Eng* **44** 220–3
- Epstein B R and Foster K R 1983 Anisotropy in the dielectric properties of skeletal muscle *Med. Biol. Eng. Comput* **21** 51–5
- Dubowitz V 1985 *Muscle Biopsy: A Practical Approach* 2nd edn (London: Bailliere Tindall) p 29
- Esper G J, Shiffman C A, Aaron R, Lee K S and Rutkove S B 2006 Assessing neuromuscular disease with multifrequency electrical impedance myography *Muscle Nerve* **34** 595–602
- Gabriel C, Gabriel S and Corthout E 1996 The dielectric properties of biological tissues: I. Literature survey *Phys. Med. Biol* **41** 2231–49
- Garmirian L P, Chin A B and Rutkove S B 2009 Discriminating neurogenic from myopathic disease via measurement of muscle anisotropy *Muscle Nerve* **39** 16–24
- Mayhew T M, Pharaoh A, Austin A and Fagan D G 1997 Stereological estimates of nuclear number in human ventricular cardiomyocytes before and after birth obtained using physical disectors *J Anat.* **191** 107–15
- Nie R, Chin A B, Lee K S, Sunmonu N A and Rutkove S B 2006 Electrical impedance myography: transitioning from human to animal studies *Clin. Neurophys* **117** 1844–9
- Polak J F, Jolesz F A and Adams D F 1988 Magnetic resonance imaging of skeletal muscle. Prolongation of T1 and T2 subsequent to denervation *Invest Radiol.* **23** 365–9
- Rutkove S B 2009 Electrical impedance myography: background, current state, and future directions *Muscle Nerve* at press
- Rutkove S B, Aaron R and Shiffman C A 2002 Localized bioimpedance analysis in the evaluation of neuromuscular disease *Muscle Nerve* **25** 390–7
- Rutkove S B, Esper G J, Lee K S, Aaron R and Shiffman C A 2005 Electrical impedance myography in the detection of radiculopathy *Muscle Nerve* **32** 335–41

- Rutkove S B, Zhang H, Schoenfeld D A, Raynor E M, Shefner J M, Cudkowicz M E, Chin A B, Aaron R and Shiffman C A 2007 Electrical impedance myography to assess outcome in amyotrophic lateral sclerosis clinical trials *Clin. Neurophysiol* **118** 2413–8
- Tarulli A, Esper G J, Lee K S, Aaron R, Shiffman C A and Rutkove S B 2005 Electrical impedance myography in the bedside assessment of inflammatory myopathy *Neurology* **65** 451–2
- Wessig C, Koltzenburg M, Reiners K, Solymosi L and Bendszus M 2004 Muscle magnetic resonance imaging of denervation and reinnervation: correlation with electrophysiology and histology *Exp. Neurol* **185** 254–61